

# Stepwise phase modulation of recoilless gamma radiation in a coincidence experiment: Gamma echo

Ilkka Tittonen, Mikk Lippmaa, Panu Helistö, and Toivo Katila

*Department of Technical Physics, Helsinki University of Technology, SF-02150 Espoo, Finland*

(Received 22 September 1992)

Classical phase-modulation theory is applied to describe the interference of the recoil-free gamma-radiation fields emitted by a Mössbauer source and a resonant absorber in forward-scattering geometry. During the exponential decay of the excited state in the source the resonant absorber develops and emits a coherent field, which interferes destructively with the source field. A stepwise phase change of the source field relative to the absorber field is introduced by a fast mechanical displacement of the source. As a result, an intense pulse of gamma rays is observed in the time dependence of the resonantly filtered radiation. This coherent transient phenomenon is called a gamma echo. The time reference of the gamma-echo experiment is the moment of formation of the excited state in the source. This is in contrast to earlier transient Mössbauer experiments in which the measurements were synchronized to the phase of the modulation and averaging occurred over all possible times of formation of the excited state. By choosing a suitable shape for the phase-modulation function in the echo experiment, short pulses of gamma radiation with desired duration and amplitude can be generated within a time frame defined by the lifetime of the excited nuclear state. Here, a detailed description of the experimental and theoretical aspects of stepwise phase modulation in a coincidence scheme is given. Theoretical results are presented in a general form, taking into account the experimental nonidealities. The properties of the mechanical drive system are discussed in detail. Gamma-echo data are presented. Good agreement between the theoretical calculations and the experimental data has been established.

## I. INTRODUCTION

We describe an interference phenomenon of coherent gamma-radiation fields, where a phase-modulated radiation field from a Mössbauer source is used to generate a secondary field in a resonant absorber and the interference of these two fields is observed. This phenomenon can be observed in a time domain experiment in which the measurement is synchronized to the formation of the 14.4-keV  $^{57}\text{Fe}$  Mössbauer state employing conventional delayed coincidence techniques. At a certain time during the decay of the excited state, the source is shifted by a distance comparable to the wavelength of the gamma radiation. The resulting phase change causes constructive interference between the source and absorber fields to appear. This interference phenomenon was described in Ref. 1. The time dependence of the gamma-radiation field of the Mössbauer source and the influence of the resonant absorber on the transmitted radiation are treated classically.<sup>2-4</sup> In this publication, a detailed description of the mechanical construction of the phase-modulation drive used in the gamma-echo experiment is given. The influence of the resonant absorber on the time distribution of the transmitted gamma rays (time filtering) is studied in detail, since the resulting curve forms the background of the echo signal. The calculations are performed in a general form, taking into account the influence of line broadenings, center shifts, and the finite rise time of the stepwise phase-modulation function.

Results of the time dependence of resonantly filtered gamma rays were presented in 1960 by Lynch, Holland,

and Hamermesh.<sup>5</sup> The time distribution of gamma rays transmitted through a resonant absorber was described by a theory in which each Fourier component of the incident radiation is changed in amplitude and phase according to a complex index of refraction. The incident wave was modified by coherently scattered waves from the harmonic oscillators within the absorber. A quantum mechanical treatment resulted in identical results.<sup>6</sup>

The early applications of the classical theory were related to delayed-coincidence measurements in the velocity domain. The experimental linewidth could be reduced by time gating because only those gamma rays were collected that are registered late after the formation of the excited state, resulting in a better defined energy. Neuwirth performed time-gated measurements with several fixed delays and obtained considerably better agreement between theory and experiment with short delays compared with the longer delays.<sup>7</sup> Hamill and Hoy<sup>8</sup> improved the method by integrating the time dependence over the experimental time window and a relatively good agreement between the theory and the experimental data was established. They could also show that the integration resulted in an expression of the transmission integral, already known from the work of Marguelies and Ehrman.<sup>9</sup> Triftshäuser and Craig applied this method to studies of  $^{57}\text{Fe}$  chemical charge states in the source experiments of several compounds.<sup>10</sup>

Experiments related to the time-dependent phenomena of gamma radiation and complementary to the gamma-echo studies have been carried out by Shvyd'ko, Smirnov, and Popov.<sup>11</sup> Instead of measuring the interfer-

ence phenomena in a forward-scattering geometry, they were able to cut off the original source radiation, enabling studies of the secondary absorber radiation only. For this purpose they used single-crystal  $^{57}\text{FeBO}_3$  polarization shutters that could be controlled by external magnetic fields.

## II. THEORY

The time-dependent part of the classical recoilless radiation field of a single line source is described as  $E_s(t, t_0) \propto e^{-\Gamma_0 t/2 + i\omega_s t + i\varphi(t)} \Theta(t)$ , where  $\Gamma_0$  is the natural linewidth, the time of formation of the excited state is  $t_0 = 0$ ,  $\omega_s$  is the angular frequency corresponding to the gamma transition energy  $\hbar\omega_s$ ,  $\varphi(t)$  describes the phase modulation, and  $\Theta(t)$  is the step function. In the experiments presented here, polarization was not determined and need not be specified. The propagation of the source field through the resonantly absorbing material can be calculated as a convolution integral of the absorber response<sup>12</sup>  $a(t) = \delta(t) - be^{i\omega_a t - \Gamma_a t/2} \sigma(bt) \Theta(t)$  and  $E_s(t)$ . The center shift between the absorber and the source is  $\Delta\omega = \omega_a - \omega_s$ ,  $\Gamma_a$  is the linewidth of the absorber, and  $\sigma(bt) = J_1(2\sqrt{bt})/\sqrt{bt}$ , where  $J_1$  is the ordinary Bessel function of the first kind, and  $b = T_a \Gamma_0/4$ , where  $T_a$  is the Mössbauer thickness of the absorber.

Because of the delta function in the absorber response,

the transmitted recoilless field can be written as a sum of the original source field and the field developed by the absorber,  $E_T(t) = \int_{-\infty}^{\infty} E_s(t-t')a(t')dt' = E_s(t) + E_a(t)$ . The absorber field is

$$E_a(t) = -be^{-\Gamma_0 t/2 + i\omega_s t} \int_0^t e^{i\Delta\omega t' - \gamma_a t'/2 + i\varphi(t-t')} \times \sigma(bt') \Theta(t-t') dt'. \quad (1)$$

The broadening of the absorber resonance line has been included here by assuming that the line remains Lorentzian in shape. In this case the absorber linewidth  $\Gamma_a$  can simply be written in the form  $\Gamma_a = \Gamma_0 + \gamma_a$ , where  $\gamma_a$  is the additional broadening. In case the source linewidth is greater than the natural linewidth, the calculation of the transmission intensity becomes more complicated as explained in Ref. 1.

In the experiments described here a stepwise phase change of the source radiation field during the decay of the excited state is used. In an ideal case, the phase change can be described by a step function

$$\varphi(t) = \Delta\varphi \Theta(t - t_1), \quad (2)$$

where  $\Delta\varphi$  is a constant and  $t_1$  is the moment of the phase change. In calculating the resonant part of the transmitted intensity using the phase modulation of Eq. (2), the following result can be derived:

$$\begin{aligned} |E_T(t)|^2 = & e^{-\Gamma_a t} \left| \sum_{k=0}^{\infty} J_k(2\sqrt{bt})(-\beta\sqrt{bt})^k \right|^2 \Theta(t) \\ & + 2e^{-\Gamma_a t + \gamma_a t_1} (1 - \cos \Delta\varphi) \left| \sum_{k=0}^{\infty} J_k[2\sqrt{b(t-t_1)}][-\beta\sqrt{b(t-t_1)}]^k \right|^2 \Theta(t-t_1) \\ & - \left\{ e^{-\Gamma_a t + \gamma_a t_1/2 + i\Delta\omega t_1} (1 - e^{-i\Delta\varphi}) \left[ \sum_{k=0}^{\infty} J_k(2\sqrt{bt})(-\beta\sqrt{bt})^k \right] \right. \\ & \quad \left. \times \left[ \sum_{n=0}^{\infty} J_n[2\sqrt{b(t-t_1)}][-\beta^* \sqrt{b(t-t_1)}]^n \right] \Theta(t-t_1) + \text{c.c.} \right\}. \quad (3) \end{aligned}$$

In the above equation,  $\beta = (i\Delta\omega - \gamma_a)/b$ . The series of the form  $\sum_{k=0}^{\infty} J_k(2\sqrt{x})(-\beta\sqrt{x})^k$  converge when  $|\beta\sqrt{x}| < 1$ . If  $|\beta\sqrt{x}| > 1$ , the expression  $e^{1/\beta - \beta x} - \sum_{k=1}^{\infty} (\beta\sqrt{x})^{-k} J_k(2\sqrt{x})$  should be used instead. If  $\beta = 0$ , i.e.,  $\Delta\omega = 0$  and  $\gamma_a = 0$ , a rather simple expression is obtained:

$$|E_T(t)|^2 = e^{-\Gamma_0 t} J_0^2(2\sqrt{bt}) \Theta(t) + 2e^{-\Gamma_0 t} (1 - \cos \Delta\varphi) \{ J_0^2[2\sqrt{b(t-t_1)}] - J_0(2\sqrt{bt}) J_0[2\sqrt{b(t-t_1)}] \} \Theta(t-t_1). \quad (4)$$

It is seen that the first terms of Eqs. (3) and (4) describe the "time filtering" by the absorber of the exponentially decaying source gamma radiation with no phase modulation. The rest of the equations describes the influence of the phase step, i.e., gamma echo. The echo amplitude is directly proportional to the term  $(1 - \cos \Delta\varphi)$  and thus the phase step of  $\Delta\varphi = \pi$  gives the maximum echo intensity. The time dependence of the echo signal resembles the filtered decay with no phase modulation, but it is delayed by the time  $t_1$ .

In the experiments, the phase step can be produced

by displacing the source relative to the absorber with a piezoelectric transducer and then the influence of a finite rise time of the phase change must also be taken into account in the calculations. The integral of Eq. (1) can be evaluated analytically if the function  $\varphi(t)$  is at least piecewise linear in time. Here, we approximate the finite rise time of the phase change by a model which consists of  $n$  consecutive linear intervals. The shape of the phase change is thus defined by the constants  $\varphi_1, \dots, \varphi_n$  corresponding to times  $t_1, \dots, t_n$  so that when  $t_i < t < t_{i+1}$  the phase change is

$$\varphi(t) \approx \varphi_i + \frac{\varphi_{i+1} - \varphi_i}{t_{i+1} - t_i}(t - t_i). \quad (5)$$

We impose an additional restriction that  $\varphi_0 = \varphi_1 = 0$  and when  $t > t_n$ ,  $\varphi(t) = \varphi_n$ . The shape of the function  $\varphi(t)$  is shown in Fig. 1. We shall use the following definitions:

$$\begin{aligned} \dot{\varphi}_i &= \frac{\varphi_{i+1} - \varphi_i}{t_{i+1} - t_i}, \\ \alpha_i &= \frac{1}{b} \left( i(\dot{\varphi}_i - \Delta\omega) + \frac{\gamma_a}{2} \right), \\ \alpha_{-1} &= 0. \end{aligned} \quad (6)$$

After evaluating the integral in Eq. (1) we get

$$\begin{aligned} E_a(t) = e^{i\omega_a t - \Gamma_a t/2} & \left[ \sum_{s=0}^{\infty} J_s(2\sqrt{bt})(\alpha_0\sqrt{bt})^s \Theta(t) - e^{\alpha_0 b t_1} \sum_{s=0}^{\infty} J_s[2\sqrt{b(t-t_1)}][\alpha_0\sqrt{b(t-t_1)}]^s \Theta(t-t_1) \right. \\ & + e^{i\varphi_1 + \alpha_0 b t_1} \sum_{s=0}^{\infty} J_s[2\sqrt{b(t-t_1)}][\alpha_1\sqrt{b(t-t_1)}]^s \Theta(t-t_1) \\ & - e^{i\varphi_2 + \alpha_0 b t_2} \sum_{s=0}^{\infty} J_s[2\sqrt{b(t-t_2)}][\alpha_1\sqrt{b(t-t_2)}]^s \Theta(t-t_2) + \dots \\ & + e^{i\varphi_{n-1} + \alpha_0 b t_{n-1}} \sum_{s=0}^{\infty} J_s[2\sqrt{b(t-t_{n-1})}][\alpha_{n-1}\sqrt{b(t-t_{n-1})}]^s \Theta(t-t_{n-1}) \\ & - e^{i\varphi_n + \alpha_0 b t_n} \sum_{s=0}^{\infty} J_s[2\sqrt{b(t-t_n)}][\alpha_{n-1}\sqrt{b(t-t_n)}]^s \Theta(t-t_n) \\ & \left. + e^{i\varphi_n + \alpha_0 b t_n} \sum_{s=0}^{\infty} J_s[2\sqrt{b(t-t_n)}][\alpha_0\sqrt{b(t-t_n)}]^s \Theta(t-t_n) - e^{i\varphi_n} \right]. \end{aligned} \quad (7)$$

We can now write a more compact expression for the observed intensity,

$$\begin{aligned} I(t) &= |E_T(t)|^2 = |E_s(t) + E_a(t)|^2 \\ &= e^{-\Gamma_a t} \left| \sum_{k=0}^n e^{\alpha_0 b t_k + i\varphi_k} \Theta(t-t_k) \sum_{s=0}^{\infty} J_s[2\sqrt{b(t-t_k)}][\sqrt{b(t-t_k)}]^s (\alpha_k^s - \alpha_{k-1}^s) \right|^2. \end{aligned} \quad (8)$$

By using this equation the influence of any experimental phase change can be analyzed by modeling  $\varphi(t)$  with piecewise linear intervals.

The observed intensity consists of resonant and non-resonant radiation components  $I(t) = f_s |E_T(t)|^2 + (1 - f_s) |E_s(t)|^2$ , where  $f_s$  is the recoilless fraction of the source. The influence of the experimental setup on the measured intensity can be taken into account by calculating the convolution integral of the time resolution function and  $I(t)$ .<sup>13</sup>

In the following, theoretical results are presented for the  $^{57}\text{Fe}$  resonance assuming a single line source and absorber. The characteristic decay constant is the natural linewidth. The influence of the finite rise time of the phase-modulation function on the transmitted intensity is shown in Fig. 2. It is assumed that a value  $\Delta\varphi = \pi$  is reached in 10 ns [Fig. 2(a)], in 50 ns [Fig. 2(b)], or in 100 ns [Fig. 2(c)] ( $f_s = 1$ ,  $\gamma_a = 0$ , and  $\Delta\omega = 0$ ). Here the time of formation of the excited state of  $^{57}\text{Fe}$  is  $t_0 = 0$ . In the transmission intensity, nonexponential behavior can be seen after  $t_0$ . Corresponding to the linear phase change during  $t_1$  and  $t_1 + \Delta t$ , echo signals are obtained. In order to observe a very pronounced echo signal, the rise time must typically be on the order of 10 ns, but the phenomenon can still be observed if the rise time is even 10 times longer.

In Fig. 3 the influence of the center shift  $\Delta\omega$  on the gamma-echo curves is shown. In the calculated examples  $\Delta\omega = 0, 5$ , or  $10 \Gamma_0$  ( $T_a = 10$ ,  $\Delta\varphi = \pi$ , and  $f_s = 1$ ). As the shift  $\Delta\omega$  increases, the echo signal becomes weaker, but additional well-resolved oscillations in intensity appear [Figs. 3(b) and 3(c)].

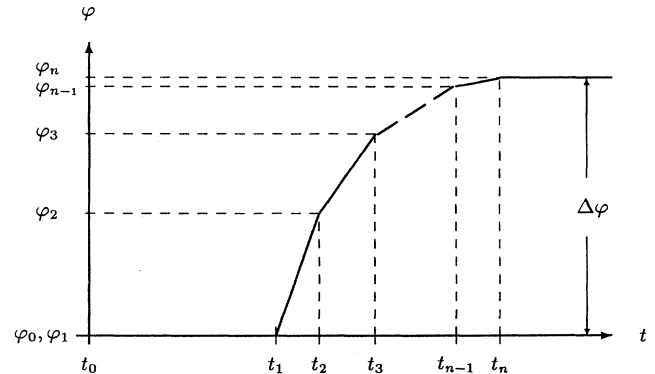


FIG. 1. Solid curve describes the shape of the modeled phase-modulation function. The symbol  $t_0$  is the time of formation of the excited state. A phase change of  $\Delta\varphi$  is reached after the rise time of  $\Delta t = t_n - t_1$ .

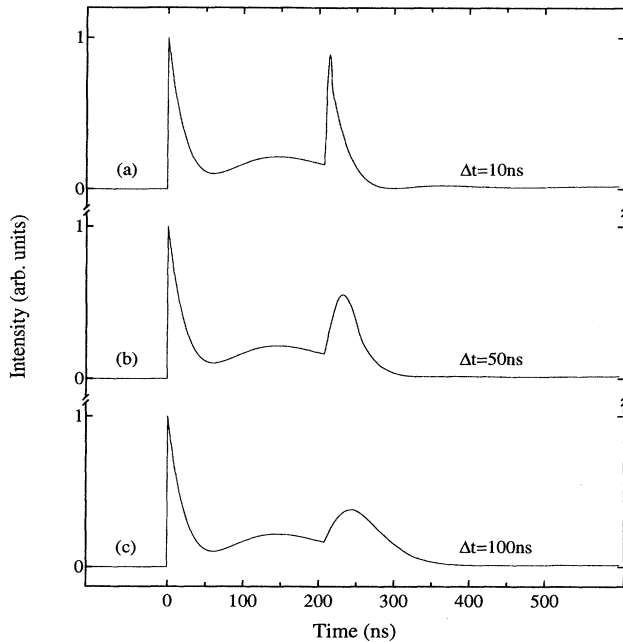


FIG. 2. Influence of the phase change from 0 to  $\Delta\varphi = \pi$ , resulting from a linear rise time between  $t_1$  and  $t_1 + \Delta t$ . The calculation has been performed for (a)  $\Delta t = 10$  ns, (b)  $\Delta t = 50$  ns, and (c)  $\Delta t = 100$  ns ( $t_1 = 3.67/b = 207$  ns,  $f_s = 1.0$ ,  $T_a = 10$ , and  $\Delta\omega = 0$ ).

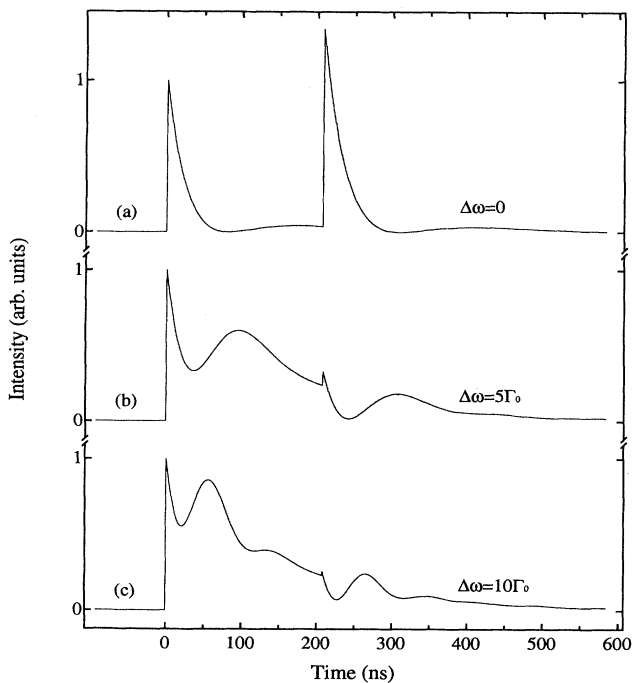


FIG. 3. Theoretical gamma-echo curves with various center shifts. The amplitude of a stepwise ( $\Delta t = 0$ ,  $t_1 = 207$  ns) phase change is  $\Delta\varphi = \pi$  and a relatively thick absorber of  $T_a = 10$  is assumed. The center shift values are  $\Delta\omega = 0, 5$ , and  $10\Gamma_0$  corresponding to the (a), (b), and (c), respectively.

### III. EXPERIMENTAL

The experimental setup was based on an ordinary delayed coincidence scheme usually used in measurements of the lifetimes of nuclear states. The schematic layout of the whole measurement setup is shown in Fig. 4. In our experiment, a  $1\text{-mm}^2$  piece of a  $6\text{-}\mu\text{m}$ -thick  $^{57}\text{Co}:Rh$  source was mounted on a polyvinylidene fluoride (PVDF) plastic piezoelectric transducer (thickness  $9\text{ }\mu\text{m}$ ). The rise time of the driving electric pulse was below 15 ns. In the measurements of the filtered decay of the source radiation, resonant  $^{57}\text{Fe}_{0.1}\text{Rh}_{0.9}$  absorbers with thicknesses of either 6 or  $12\text{ }\mu\text{m}$  were used. The moment of formation of the Mössbauer state was determined by detecting the 122.1-keV gamma rays. In the start channel detector a 1.5-cm-thick plastic scintillator was bonded to either a Philips XP-2020-Q or a Hamamatsu R2076 photomultiplier. Lower-energy gamma rays were filtered out with a 3-mm-thick aluminum layer (transmission for the 14.4-keV gamma rays is on the order of 0.1%). The fast anode pulse from the detector was amplified with a fast timing amplifier and fed into a constant fraction discriminator. The timing pulse from the discriminator was used to produce a start signal to the time analyzer (TAC) and to trigger the pulse generator giving a fast voltage step across the piezoelectric transducer after a certain time delay.

The 14.4-keV gamma quanta were detected with an integrated detector system containing a 0.1-mm-thick NaI crystal. A leading-edge (LE) discriminator was used to derive a time-pickoff signal from the fast anode pulses of the detector. Those pulses were used to give the stop pulse to the time analyzer. To optimize the time resolution, the discriminator level had to be set very close to the noise level. The analog output signal of the time analyzer was connected to the Afora LPD 7014 pulse height analyzer (PHA). The gate pulse for the pulse height analyzer was obtained from the last dynode of the NaI detector.

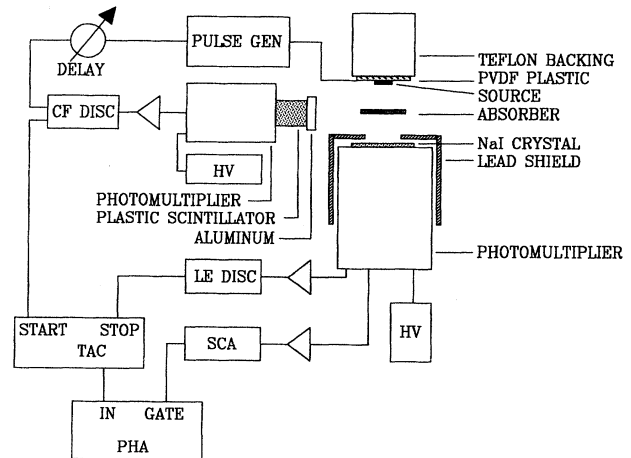


FIG. 4. Schematic layout of the experimental setup used in the gamma-echo measurements. The timing pulse of the START channel detector is also used to trigger the pulse generator which is connected to the drive unit. Absorber is placed between the source and the STOP channel detector.

The slow pulses were amplified with a spectroscopy amplifier and a single-channel analyzer (SCA) was used to select the pulses corresponding to the 14.4-keV transition. The two detectors were positioned at an approximately 90° angle to each other and shielded with lead to prevent scattering of x rays.

The detailed drawing of our source holder is given in Fig. 5. The piezoelectric drive was built on a Teflon backing. Several materials were tested and Teflon was selected because of similar acoustic properties with PVDF. The Teflon base was approximately 30 mm long to prevent reflected waves from the bottom of the base from reaching the PVDF foil during a decay event. A 20-mm-long and 3-mm-wide strip of 9- $\mu\text{m}$  PVDF foil was glued onto the Teflon base with a thin layer of epoxy glue. The aluminum coating of the PVDF foil was etched in such a way that a small overlapping area of approximately 5 mm<sup>2</sup> was left at the center where the source was glued. The conversion factor between the voltage and the phase amplitude was found to depend strongly on the construction of the drive and not only on the thickness of the PVDF foil. The delay between the start of the decay process and the generation of the echo pulse could be adjusted from 100 ns to 1  $\mu\text{s}$ .

The time resolution of the measurement system was checked with an <sup>88</sup>Y source (the coincident gamma- and x-ray energies were 1.2 MeV and 14.1 keV). It was found that the resulting time resolution function is slightly non-Gaussian [full width at half maximum (FWHM)=5 ns] with a small asymmetry due to an exponential tail. In addition, 25- and 40- $\mu\text{m}$ -thick PVDF foils and 0.3-mm-thick LiNbO<sub>3</sub> and quartz crystals were tested, but source movement was of slightly worse quality due to spurious vibrations after the fast voltage step. The time resolution of 5.5(1) ns was also obtained by fitting the lifetime spectra assuming a Gaussian distribution for the time resolution function. To obtain comparative information about the Mössbauer parameters of both the source and the absorber, conventional measurements were also performed in a transmission geometry.

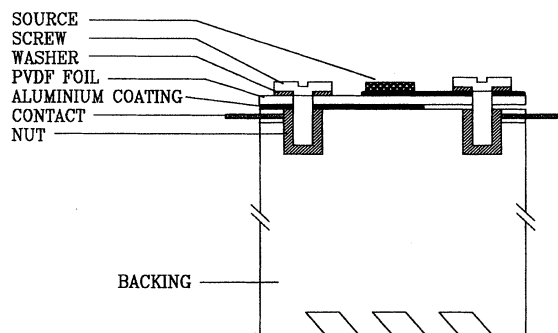


FIG. 5. Detailed drawing of the source holder. The source foil is glued on the PVDF piezoelectric foil and special care was taken to attach the foil rigidly to the Teflon backing.

#### IV. EXPERIMENTAL RESULTS

When no resonant absorber was used in the experimental setup, an exponential decay was observed. A value of  $1/\Gamma_0=140(2)$  ns for the lifetime of the 14.4-keV state of <sup>57</sup>Fe was obtained from the fit with a single exponential assuming a linear background and a Gaussian time resolution function.

In Fig. 6(a) the filtered decay through a 6- $\mu\text{m}$ -thick <sup>57</sup>Fe<sub>0.1</sub>Rh<sub>0.9</sub> foil is shown. The shape of the curve was reproduced using the classical theory [ $\varphi(t)=0$ ]. According to the fit, the recoilless fraction of the <sup>57</sup>Co:Rh source was  $f_s=0.76(1)$ . The absorber linewidth appeared broadened with  $\Gamma_a = 1.7(2)\Gamma_0$ . The center shift was zero. In the measurement shown in Fig. 6(b), the 12- $\mu\text{m}$ -thick absorber was used. It is seen that in the resulting curve the observed decay is even faster and that the influence of the delayed absorber field becomes more prominent. According to the analysis based on Eq. (3)  $f_s=0.768(3)$ ,  $\Gamma_a=1.48(3)\Gamma_0$ , and  $T_a=13.7(2)$ .

Mössbauer spectra of the <sup>57</sup>Fe<sub>0.1</sub>Rh<sub>0.9</sub> absorbers in the velocity domain were analyzed using the transmission integral method.<sup>9</sup> The values obtained for the source and the absorber linewidths were closer to the natural linewidth than those revealed by the analysis of the time domain measurements:  $\Gamma_s + \Gamma_a = 2.16(6)\Gamma_0$ . The recoilless fraction of the source appeared to be  $f_s = 0.77(1)$  and the Mössbauer thickness of the 6- $\mu\text{m}$ -thick absorber was  $T_a=7.26(7)$ , instead of  $13.7/2=6.85$  expected from filtered decay on the 12- $\mu\text{m}$  sample. It can be concluded that the coincidence measurements of the filtered de-

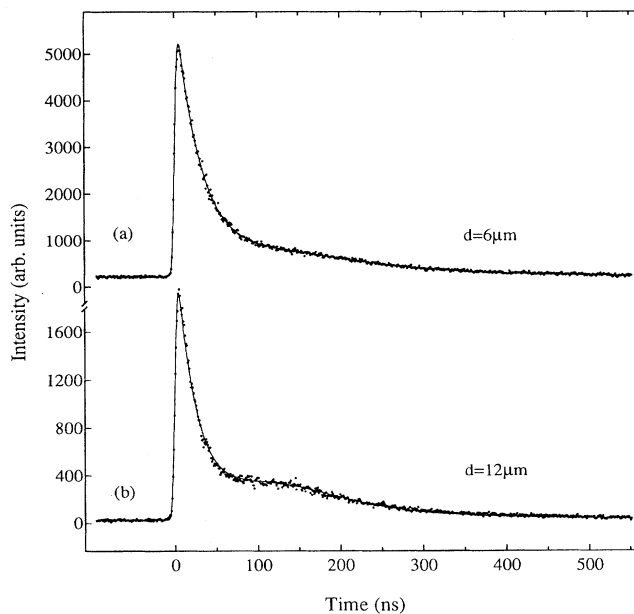


FIG. 6. Experimental <sup>57</sup>Fe coincidence curves of the filtered decay of the 14.4-keV Mössbauer state. The absorber thickness was (a) 6  $\mu\text{m}$  and (b) 12  $\mu\text{m}$ .

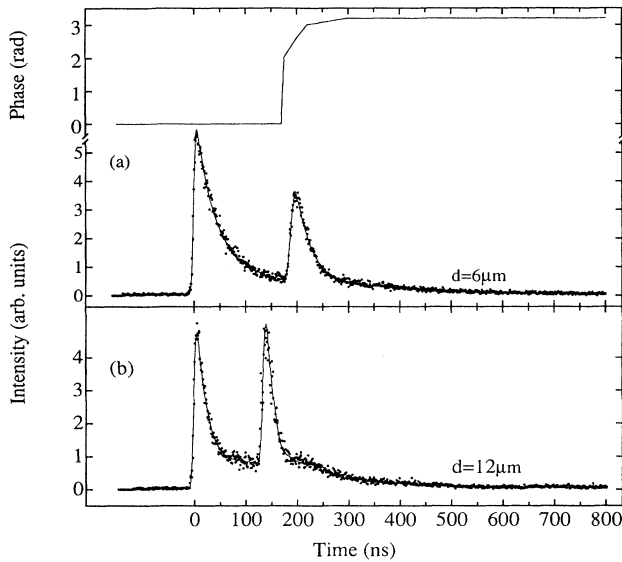


FIG. 7. Experimental gamma-echo curves: (a) a  $^{57}\text{Fe}_{0.1}\text{Rh}_{0.9}$  foil of  $6\ \mu\text{m}$  thickness ( $T_a \approx 7$ ) and (b)  $12\ \mu\text{m}$  ( $T_a \approx 14$ ) was used. The shape of the modeled phase change corresponding to (a) is also shown.

can give very accurately the recoilless fraction, but the linewidths are not easily determined with good accuracy.

Results of gamma-echo measurements using  $9\text{-}\mu\text{m}$  PVDF transducers are presented in Figs. 7 and 8. All these curves were fitted applying Eq. (8) and the shape of the experimental phase modulation step was approximated with  $\varphi(t)$  consisting of three linear intervals. Both the phase change  $\Delta\varphi$  and rise time  $\Delta t$  were fitted. The influence of the absorber thickness is studied in Fig. 7 with a  $6\text{-}\mu\text{m}$ -thick [Fig. 7(a)] and a  $12\text{-}\mu\text{m}$ -thick [Fig. 7(b)] absorbers. A voltage step of 7 V was applied across the transducer and according to the fit a phase change of

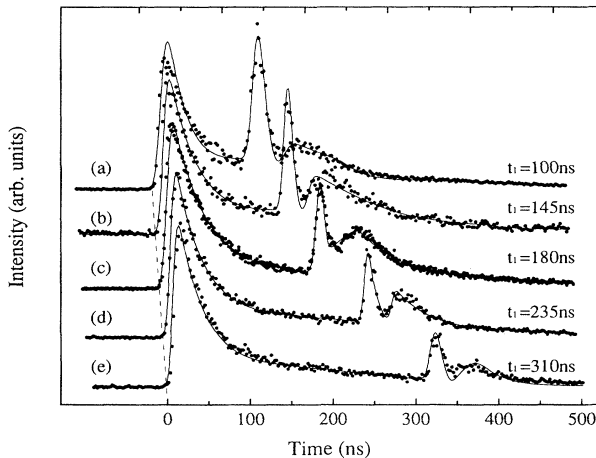


FIG. 8. Influence of the delay  $t_1$  between the time of formation of the excited state and the start of the phase modulation on experimental gamma-echo curves is shown.

$3.2(1)$  rad was produced. The shape of the phase modulation as a result of the single displacement of the source after a constant delay is shown in the upper part of the figure. It is clearly seen that as the absorber thickness is increased the decay of the echo signal appears more accelerated and the amplitude of the echo increased as well.

Figure 8 demonstrates the influence of the adjustable delay on the relative intensity of the echo signal. These curves were obtained with an output of 14 V from the pulse generator on the PVDF transducer to obtain a high amplitude for the phase change. For this reason a second maximum in the echo pulse is clearly visible as the phase change exceeds the value of  $\pi$ . The total amplitude for  $\Delta\varphi$  was  $7.5(3)$  rad, achieved in approximately 30 ns. As the delay is increased, the intensity of the echo pulse is strongly reduced, but can still be observed, even at times when the transmission intensity has almost died out. In Fig. 8(a) the height of the echo pulse even exceeds the transmission intensity at  $t = t_0$ . The delay times between the formation of the excited state and the generation of the voltage step were adjusted from 100 to 310 ns in Figs. 8(a)–8(e). It should be noted that more than one echo can be generated during a single decay event as was reported in Ref. 13.

## V. DISCUSSION

When the decay of the 14.4-keV state is observed through a resonant absorber, the intensity dies out faster than what would be observed without the absorber. This occurs due to the time filtering of source radiation by the absorber. In the classical field picture at  $t = t_0$  the absorber transmits nearly all of the incident radiation. After  $t_0$  the resonant absorber starts to develop a secondary field of its own, which interferes destructively with the source field, causing a fast drop of transmitted intensity. By applying a rapid phase change to the source field relative to the absorber field, constructive interference can be restored until rephasing of the absorber field occurs and the transmitted intensity is seen to drop again.

The time dependence of the filtered decay was found to differ slightly from that expected theoretically. Especially, an accurate determination of the absorber linewidth was difficult. It was seen that as the absorber thickness was increased the agreement between theory and experiment was improved.

The determination of Mössbauer parameters from time spectra offers several advantages over conventional methods. The use of coincidence techniques in measuring the filtered decay of the excited state is a suitable method for determining the recoilless fraction  $f_s$ . Usually the number of background pulses can be kept very low and thus the recoilless part of the gamma radiation can be determined with high accuracy since a signal-to-noise correction is not needed. Also the Mössbauer thickness  $b$  and the absorber linewidth  $\Gamma_a$  can in principle be independently analyzed.

In all transient Mössbauer experiments the construction of the drive system is of great importance in order to produce a phase modulation of high quality. Sev-

eral piezoelectric transducer materials can be used. We found the 9- $\mu\text{m}$ -thick PVDF (polyvinylidene fluoride) foil very suitable to our experiments with  $^{57}\text{Fe}$ . The PVDF foils have successfully been used earlier in transient Mössbauer experiments<sup>14</sup> and as ultrasonic filters.<sup>15,16</sup> The way the PVDF foil was attached on the backing seemed to influence strongly the conversion factor. In the construction of the drive the use of a proper backing block was essential to minimize spurious vibrations after the sudden displacement. The slight discrepancies between the fits and the experimental echo curves presented were due to these vibrations. Additional experimental broadenings were caused by small deviations due to time jitter of the voltage step that was applied on the drive foil. Despite all these experimental restrictions analysis of the phase modulation and the corresponding motion of the source foil was possible with high accuracy, considering that a phase change of  $\Delta\varphi = \pi$  corresponds to a shift  $\Delta x = 43$  pm. The demonstration of the gamma-

echo phenomenon was indisputable.

Coherent transient effects have recently gained more interest because of the development of synchrotron radiation facilities. In such measurements, a short pulse excites a large number of resonant nuclei in a sample simultaneously and the time dependence of the resulting decay signal is measured. In principle, the gamma-echo formalism and method should also be applicable in synchrotron experiments, for example, in creating a delayed constructive interference signal of a strong exciting pulse.

#### ACKNOWLEDGMENTS

The authors thank Dr. E. Ikonen for valuable discussions and Dr. K. Rytsölä, Dr. J. Hietaniemi, J. Lindén, and J. Karimäki for help during the experiments. Financial support from the Emil Aaltonen Foundation is acknowledged.

<sup>1</sup>P. Helistö, I. Tittonen, M. Lippmaa, and T. Katila, *Phys. Rev. Lett.* **66**, 2037 (1991).

<sup>2</sup>G. J. Perlow, *Phys. Rev. Lett.* **40**, 896 (1978).

<sup>3</sup>J. E. Monahan and G. J. Perlow, *Phys. Rev. A* **20**, 1499 (1979).

<sup>4</sup>E. Ikonen, P. Helistö, T. Katila, and K. Riski, *Phys. Rev. A* **32**, 2298 (1985).

<sup>5</sup>F. J. Lynch, R. E. Holland, and M. Hamermesh, *Phys. Rev.* **120**, 513 (1960).

<sup>6</sup>S. Harris, *Phys. Rev.* **124**, 1178 (1961).

<sup>7</sup>W. Neuwirth, *Z. Phys.* **197**, 473 (1966).

<sup>8</sup>D. W. Hamill and G. R. Hoy, *Phys. Rev. Lett.* **21**, 724 (1968).

<sup>9</sup>S. Marguelies and J. R. Ehrman, *Nucl. Instrum. Methods* **12**, 131 (1961).

<sup>10</sup>W. Triftshäuser and P. P. Craig, *Phys. Rev.* **162**, 274 (1967).

<sup>11</sup>Yu. V. Shvyd'ko, G. V. Smirnov, and S. L. Popov, *Pis'ma Zh. Eksp. Teor. Fiz.* **53**, 69 (1991) [*JETP Lett.* **53**, 69 (1991)].

<sup>12</sup>Yu. Kagan, A. M. Afanas'ev, and V. G. Kohn, *J. Phys. C* **12**, 615 (1979).

<sup>13</sup>I. Tittonen, P. Helistö, M. Lippmaa, and T. Katila, *Hyperfine Interact.* **71**, 1465 (1992).

<sup>14</sup>P. Helistö, E. Ikonen, and T. Katila, *Phys. Rev. B* **34**, 3458 (1986).

<sup>15</sup>G. von Eynatten, E. Fukada, and K. Dransfeld, *Hyperfine Interact.* **42**, 1095 (1988).

<sup>16</sup>G. von Eynatten and K. Dransfeld, *Hyperfine Interact.* **58**, 2555 (1990).